Tetrahedron Letters 53 (2012) 1645–1651

Contents lists available at SciVerse ScienceDirect

Tetrahedron Letters

journal homepage: www.elsevier.com/locate/tetlet

# Synthesis of rhenium chelated $MAG_3$ functionalized rosette nanotubes

Alaaeddin Alsbaiee [a,b], Mustapha St. Jules [a,b], Rachel L. Beingessner [a], Jae-Young Cho [a], Takeshi Yamazaki [a,b], Hicham Fenniri [a,b,c,*]

[a] National Institute for Nanotechnology, University of Alberta, 11421 Saskatchewan Drive, Edmonton, Alberta, Canada T6G 2M9
[b] Department of Chemistry, University of Alberta, 11421 Saskatchewan Drive, Edmonton, Alberta, Canada T6G 2M9
[c] Department of Biomedical Engineering, University of Alberta, 11421 Saskatchewan Drive, Edmonton, Alberta, Canada T6G 2M9

ARTICLE INFO

*Article history:*
Received 26 October 2011
Revised 18 January 2012
Accepted 20 January 2012
Available online 28 January 2012

*Keywords:*
Rosette nanotubes
Self-assembly
Mercaptoacetyl triglycine
Metal oxide
Rhenium

ABSTRACT

Rosette nanotubes (RNTs) are discrete nanostructures self-assembled from a guanine–cytosine hybrid motif (G∧C) under aqueous conditions. These materials have substantial design flexibility and a range of applications, which are partly attributed to their diverse surface functionalization. Given the potential for interesting properties resulting from a metal-RNT construct, here we describe an oxorhenium-functionalized RNT. More specifically, we present the synthesis of a twin G∧C motif expressing the mercaptoacetyl triglycine ($MAG_3$) ligand. We then examine the chelation reaction of the $MAG_3$ with $ReOCl_3(PPh_3)_2$ and self-assemble the resulting ReO-$MAG_3$-G∧C conjugate into RNTs under DMSO and aqueous conditions.



## Introduction

Rosette nanotubes (RNTs) are biocompatible architectures generated under physiological conditions through the self-assembly of a guanine–cytosine hybrid motif (G∧C) via an entropically driven, hierarchical process (Fig. 1).[1] As a result of their ease of outer surface functionalization with covalently attached pendant groups and tunable nature of their lengths[2] and diameters,[3] there is substantial flexibility in the RNT design to tailor their properties for biomedical and other materials applications. RNTs functionalized with lysine, RGDSK or a combination of both for example, have been shown to be excellent interfacial biomaterial for osteoblast (bone cells) adhesion to titanium (Ti), for hydrogel implant materials used in bone repair,[4] and for vascular stents.[5] This may have a tremendous impact for patients who often face inflammation, infection and the need for revision surgery to replace the implant devices.

In addition to serving as interfacial materials, RNTs are also being examined as scaffolds to deliver small drug molecules and large bioactive peptides and nucleic acids. The therapeutic agents can be bound to the RNTs either covalently[1] on the surface or by passive entrapment such as by electrostatic interactions[6] with charged peptides that are already expressed on the surface or by incorporation into their inner channel.[7,8]

Along with functionalizing the RNTs with organic groups, we have also described the site-specific nucleation and growth of 1.4 nm Au NPs on the surface of the RNTs.[9] This work paved the way to the nucleation of catalytically active metal NPs and the exploration of their catalytic properties.

Given our interest in hybrid metal-RNT constructs for novel properties, here we explore the synthesis of an oxorhenium-functionalized RNT. Rhenium complexes are interesting because of their known catalytic properties, particularly in hydrogenation reactions.[10] Moreover, radioactive $^{186/188}Re$ (or its substitute technetium-99 m, $^{99m}Tc$)[11] has been extensively used as a radiolabel for bioimaging studies[12] and has also been investigated as a possible method for the in situ treatment of cancerous tissue based on high-energy β-emission.[13]

The mercaptoacetyl triglycine ($MAG_3$) ligand is a well-established tubular renal imaging ligand which forms a stable metal complex with Re or Tc. Many different bioactive molecules such as sugars,[14] immune globulins,[15] and siRNA,[16] to only name a few, have been functionalized with $MAG_3$. From a structural standpoint, this ligand contains a sulfhydryl atom typically protected with a benzoyl group that requires deprotection prior to the chelation with the Re. It also features a free carboxyl group that is not involved in chelation and can be used as a handle to link other groups via an amide bond.

In this Letter, we describe a synthetic approach in which to construct a twin-G∧C motif conjugated with $MAG_3$ (Fig. 1). We then examine the chelation reaction of twin-G∧C-$MAG_3$ motif with Re and investigate the self-assembly properties of the resulting adduct into RNTs under aqueous and DMSO conditions.

* Corresponding author. Tel.: +1 780 641 1750; fax: +1 780 641 1601.
*E-mail address:* hicham.fenniri@ualberta.ca (H. Fenniri).


doi:10.1016/j.tetlet.2012.01.090

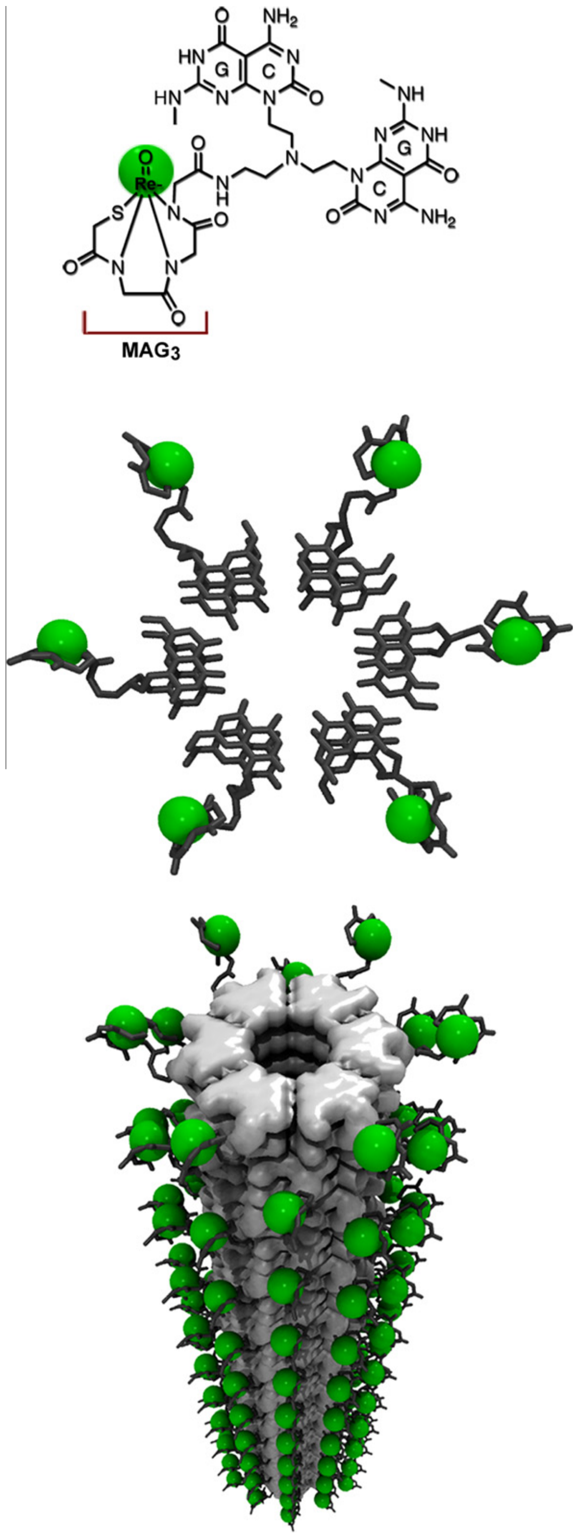


**Figure 1.** (a) Re-complexed $MAG_3$ functionalized twin G∧C motif (upper) and corresponding hexameric rosette maintained through 36 H-bonds (middle) and $\pi-\pi$ stacking of the rosettes into RNTs (lower).

## Results and discussion

### Synthesis of the $MAG_3$ functionalized twin-G∧C motif

The initial strategies that we explored to synthesize the $MAG_3$-functionalized G∧C motif are presented in Fig. 2 and commenced with the preparation of the twin-base **2** in excellent yields from aldehyde **1**[1c] and 0.5 M $NH_3$ in dioxane via a double reductive amination reaction. We then envisioned the coupling of compound **2** with readily prepared $MAG_3$ **3**[17] to generate **5** or **6**, by implementing standard peptide coupling conditions (HATU, DIPEA) or via the acid chloride, anhydride or activated carbamoylimidazolium salt **4** intermediates. As shown in Figure 2 however, all of these strategies were unproductive and only starting material was recovered. It is speculated that the limited solubility of $MAG_3$ **3** even in the polar solvent DMSO, along with steric interactions with the twin base **2** or **4**, were the main factors that prevented the coupling from taking place.

As a means of promoting the reaction by removing or at least limiting this steric impediment, the protected G∧C motifs **7** and **8** were prepared (Fig. 2). These molecules have a linker R of two or four carbon atoms respectively, along with a terminal primary amine that can be used to form an amide bond to $MAG_3$–COOR. Surprisingly however, neither the Fmoc deprotected **7** or **8** could be coupled to $MAG_3$ **3** using the conditions described previously (HATU, CDI or via the acid chloride derivative, $MAG_3$–Cl).

The order of the coupling reaction was next modified in order to take advantage of the higher reactivity of the aldehyde moiety on the G∧C protected base **1**. As illustrated in Figure 3, *N*-Boc ethylenediamine was first coupled to $MAG_3$ **3** in the presence of HBTU and $Et_3N$ in DMSO to generate amine **9** in a 77% yield. Following the removal of the Boc group on **9** under acidic conditions, a double reductive amination reaction in the presence of 2 equiv of G∧C protected base **1** and $NaBH(OAc)_3$ provided the desired coupled product **10** in a 51% yield. Global deprotection of the Boc and Bn groups using a 95% TFA in thioanisole (v:v) successfully generated the target G∧C base product **11**.

### Chelation of the $MAG_3$ functionalized twin-G∧C motif with Rhenium

With compound **11** in-hand, several typical conditions described in the literature for the Re complexation of the $MAG_3$ ligand were examined. These involved either a one-step Bz deprotection-chelation protocol or an in situ Bz deprotection under basic conditions, followed by the addition of Re in the form of $ReOCl_3(PPh_3)_2$. While various bases (NaOH[18], pyridine[19] or $Et_3N$), solvents (MeOH, DMF), temperatures (rt to 80 °C), and reaction times were examined to promote the chelation, only starting material was isolated under these conditions. Despite this unfavorable outcome, we had learned that the solubility of **11** and the Bz deprotected **11** in particular, was very limited in MeOH, which is a common solvent used for this reaction. In our case, a mixture of DMF and MeOH was a better solvent choice. As well, careful examination of the LCMS traces revealed that $ReOCl_3(PPh_3)_2$ had been oxidized to the very stable perrhenate ($ReO_4^-$)[20] anion. It was therefore evident that a normal atmosphere was also detrimental to this reaction.

Thus, taking these observations into consideration, **11** was deprotected using NaOMe in degassed MeOH[21] and then treated with a solution of $ReOCl_3(PPh_3)_2$ in DMF that was also degassed (Fig. 3). After stirring for 2 h at room temperature, diethyl ether was then added to precipitate the brown solid, which was purified by simply washing with various organic solvents. We were pleased to observe that with these measures, adduct **12** could be obtained, but unfortunately as a mixture with many other unidentified products. After extensive optimization efforts, we found that quite simply, a one-step protocol worked very well in which **11** was treated with $ReOCl_3(PPh_3)_2$ and NaOMe concurrently, in a 1:1 mixture of degassed DMF:MeOH for 30 min. The brown solid was then precipitated and washed with multiple organic solvents to provide **12** in a 94% yield. Analysis of the product by IR, $^1H$ NMR, LRMS, HRMS

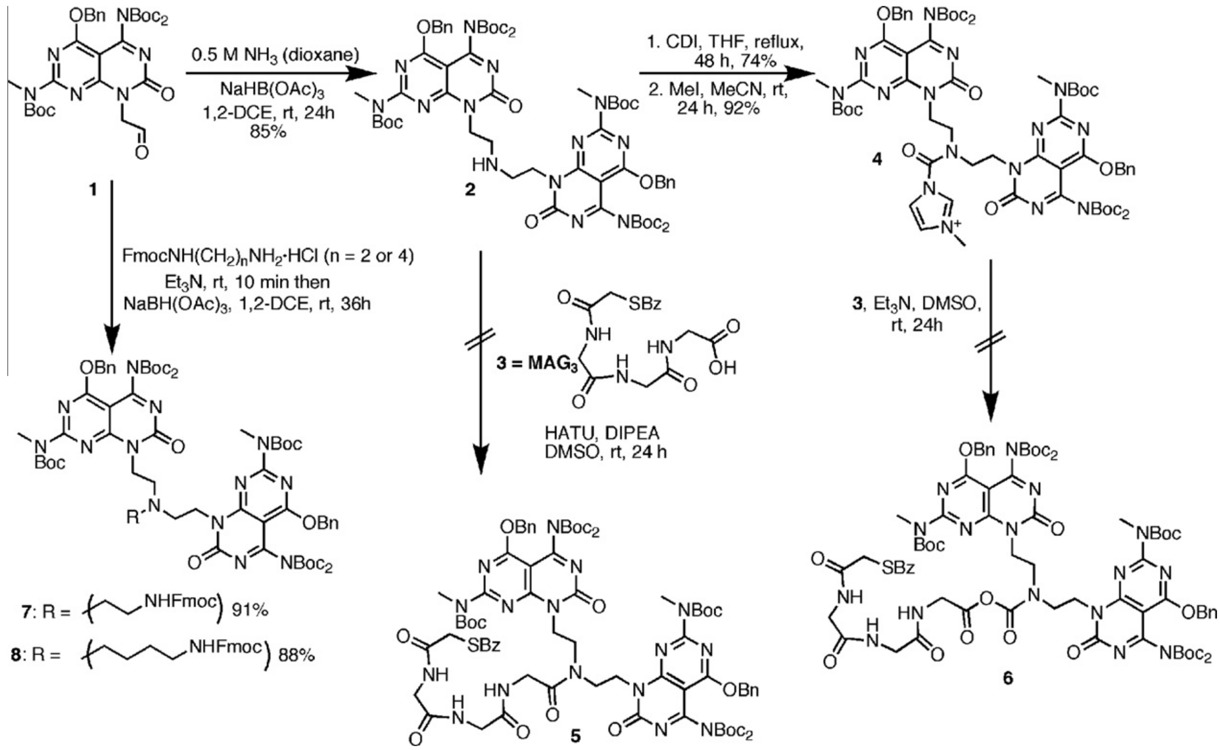

**Figure 2.** Synthetic strategies for the $MAG_3$ functionalized twin G∧C motif.

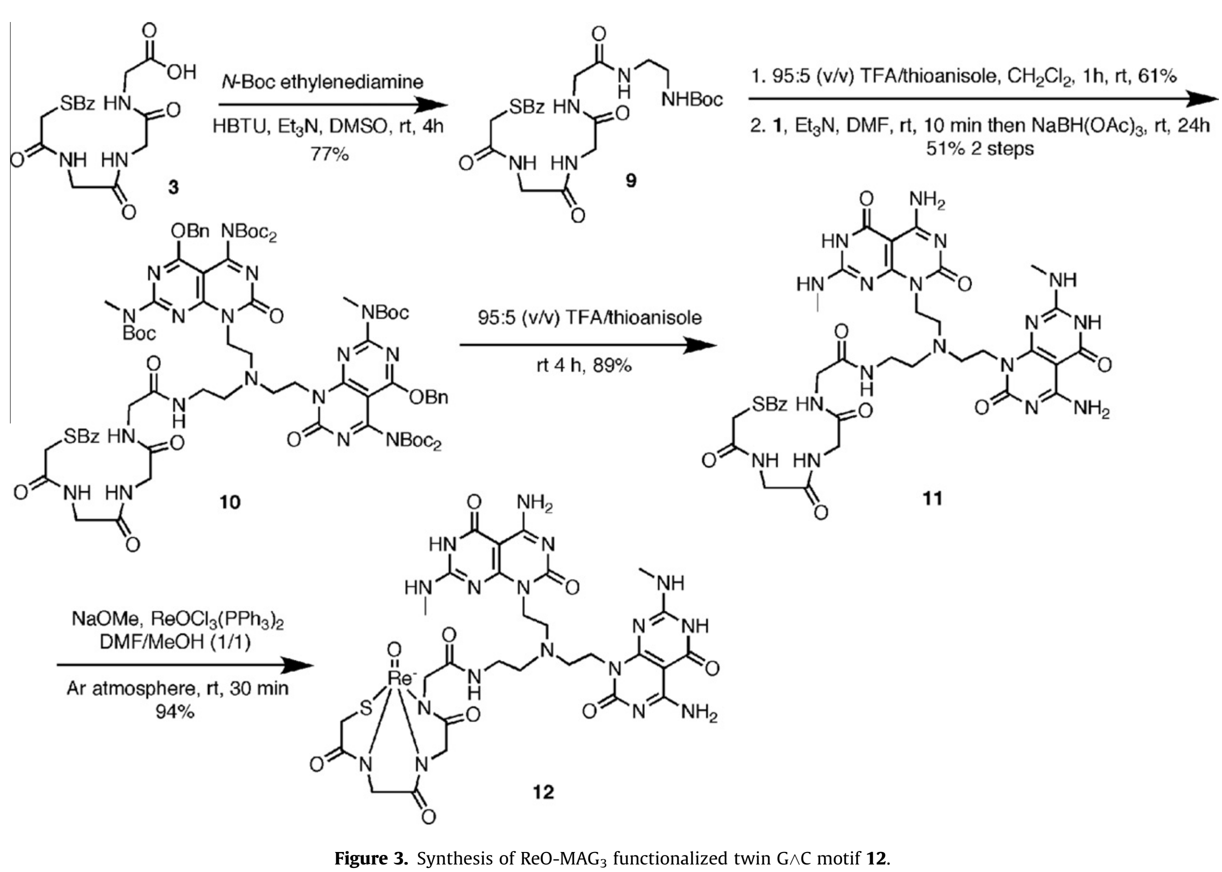

**Figure 3.** Synthesis of ReO-$MAG_3$ functionalized twin G∧C motif **12**.

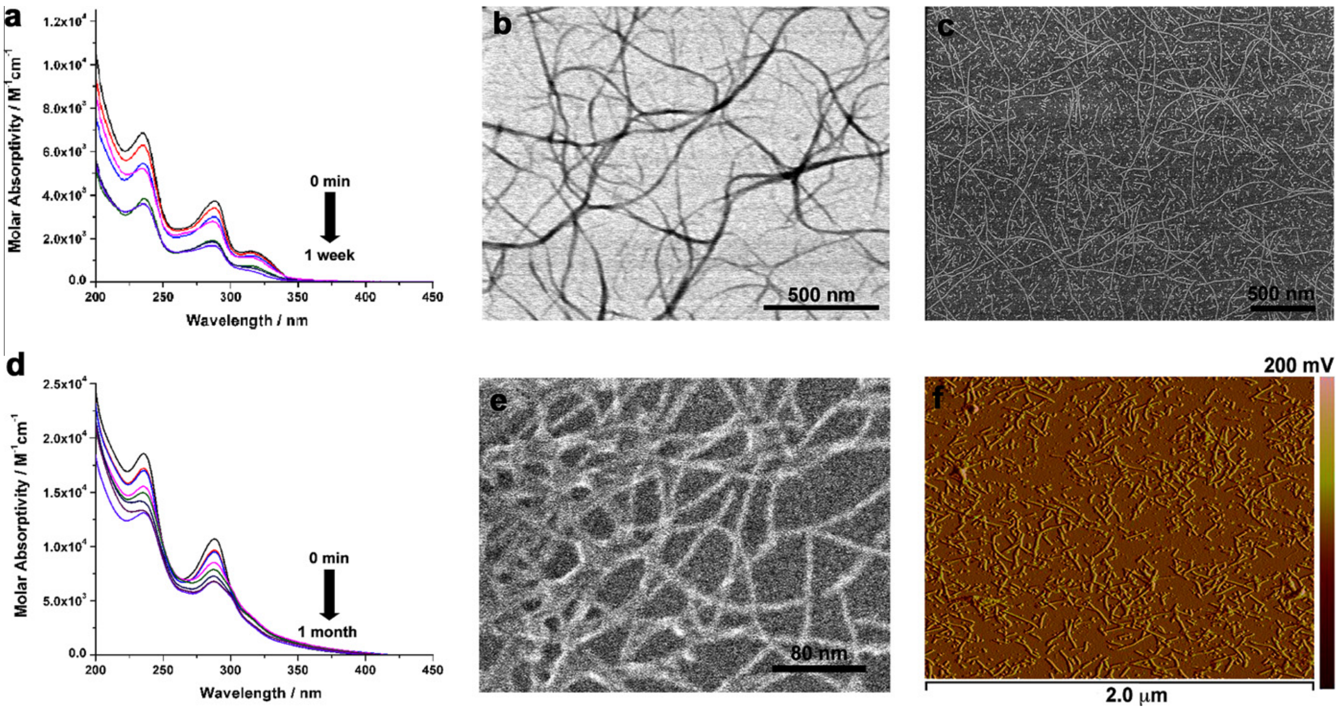


**Figure 4.** Top row–compound **11** (a) UV–Vis spectra (4.010$^{-5}$ M) monitored over time at room temperature (b) SEM (TE mode) image (1 mg/mL, water, 2 d aging) (c) SEM (SE mode) image (0.05 mg/mL, DMSO, 1 week aging). Bottom row–compound **12** (d) UV–Vis (4.8 $\times$ 10$^{-5}$ M) monitored over time at room temperature (e) SEM (SE mode) image (0.05 mg/mL, water, 1 month aging) (f) AFM image (0.05 mg/mL, DMSO, 1 week aging).

and elemental analysis established that the reaction was clean and that **12** did not require further purification.

## Self-assembly of the RNTs

The self-assembly of both the $MAG_3$-functionalized motif **11** and Re chelate **12** into RNTs was investigated, in order to determine if there was any effect of the charged metal complex on the self-organization process.

UV–Vis spectroscopy first established the absorbance profiles pertaining to the growth of the RNTs over time. As shown in Figure 4a (and Fig. S1), compound **11** ($4.0 \times 10^{-5}$ M) presents two $\lambda_{max}$ at 235 and 288 nm, which corresponds to the absorption of the $\pi-\pi$ stacked twin G∧C bases.[1] A third, less intense band at $\lambda_{max}$ of 315 nm is also observed from the benzene ring of the Bz protected $MAG_3$ ligand. During the course of one week, a hypochromic effect in the absorbance occurs, along with a small blue shift of 2 nm at the $\lambda_{max}$ 288 and 315 nm. When compared to the Re complex **12**, a similar growth absorption profile in water (Fig. 4d and Fig. S2) is found, with a hypochromic effect occurring over time at the two $\lambda_{max}$ values that range between 287–288 nm and 234–236 nm. The absence of a $\lambda_{max}$ peak at 315 nm for **12** also confirms the deprotection of the Bz group. The alternative hyperchromic effect noted during the variable-temperature UV–Vis experiments of **12** (Fig. S3), highlights the reversible nature of this self-assembly process as the system is heated.

Scanning electron microscopy (SEM, Fig. 4b, c, e, S4a, S5a), transmission electron microscopy (TEM, Figs. S4b, S5b), and atomic force microscopy (AFM, Fig. 4f, Figs. S4c, S5c) were used to further characterize the RNT assemblies. Figure 4b and e show representative SEM images of **11** (1 mg/mL) and **12** (0.05 mg/mL) in water, respectively. Although the charged metal complex leads to better solubility of **12** in water compared to **11**, the SEM images of the RNTs obtained are very similar to each other. It was also noted that for **11** and **12**, the RNTs have a tendency to associate into larger bundles. Therefore, in order to improve the dispersion of the tubes for characterization purposes, the self-assembly of the G∧C motifs were also performed in DMSO. From the corresponding TEM images of **11** (Fig. S4b) and **12** (Fig. S5b), the average RNT diameters were measured to be 4.5 ± 0.5 nm and 4.7 ± 0.4 nm respectively. Molecular modeling of RNTs **12** (Fig. S6), which were approximated by replacing the Re atom with carbon to simplify the calculations, resulted in an RNT diameter of 4.7 nm. Even though this value is only an approximation due to the replacement of the Re atom with carbon, it bodes well with our experimental values. Overall, it is evident from these studies that there is no barrier to the self-assembly process by the presence of the Re-chelated $MAG_3$ ligand in **12**.

## Conclusions

In conclusion, we have described a synthetic strategy to construct oxorhenium-functionalized RNTs using the $MAG_3$ ligand. This strategy involves a one-step deprotection-chelation protocol of **11** using NaOMe and $ReOCl_3(PPh_3)_2$ in a mixture of degassed DMF and MeOH. This provides expedient access to **12** in excellent yield and without the need for extensive purification. We have also investigated the self-assembly of **11** and **12** in DMSO and water solvents and have confirmed the formation of RNTs using UV–Vis spectroscopy, SEM, TEM, and AFM imaging. With this synthetic approach in-hand, one aspect of our future work will involve the preparation of the radiolabeled version of G∧C motif **12** using $^{186/188}$Re (or technetium-99 m, $^{99m}$Tc). This will provide a strategy in which to track the cellular uptake and pharmacokinetics of RNTs in vivo.

## Experimental

### General

All reagent grade solvents were purified using an MBraun solvent purification system. Reactions were performed under $N_2$ or Argon unless otherwise stated. Silica coated TLC plates were used to monitor reaction progress and visualization was made under UV light or by chemical staining ($KMnO_4$/dd$H_2O$ or Ninhydrin/*n*-BuOH/AcOH). All NMR characterizations were performed on a 600, 500 or 400 MHz NMR with the solvents indicated used as internal references. The NMR data are presented as follows: chemical shift, integration, multiplicity, and coupling constant.

### Compound 2

A solution of compound **1** (5.0 g, 7.8 mmol) in 1,2-dichloroethane (30 mL) was treated with 0.5 M $NH_3$ in dioxane (62.5 mL, 31.3 mmol) and NaBH$(OAc)_3$ (3.8 g, 18 mmol). After stirring at rt for 24 h, the reaction was quenched with dd$H_2O$ (20 mL). The organic phase was separated, washed with brine (10 mL), dried over anhydrous $Na_2SO_4$ and concentrated under reduced pressure (rotovap). Purification by silica gel flash chromatography provided compound **2** ($C_{62}H_{83}N_{13}O_{16}$, 4.20 g, 85%) as a yellow solid. $R_f$ = 0.2 ($SiO_2$, EtOAc). mp = 97–98 °C. $^1$H NMR (400 MHz, $CDCl_3$) $\delta$ (ppm) 7.45–7.25 (11H, m), 5.56 (4H, s), 4.42 (4H, t, *J* = 7.0 Hz), 3.47 (6H, s), 3.09 (4H, t, *J* = 7.0 Hz), 1.55 (18H, s), 1.27 (36H, s). $^{13}$C NMR (125 MHz, $CDCl_3$) $\delta$ (ppm) 165.6, 161.1, 160.2, 155.6, 152.4, 149.2, 134.9, 128.5, 127.8, 92.8, 83.6, 82.8, 69.8, 50.4, 41.0, 34.8, 28.1, 27.8. HRMS (ESI): calcd for $(M+H)^+/z$, 1266.6153. Found 1266.6150.

### Compound 4

Compound **2** (200 mg, 0.158 mmol) and *N,N'*-carbonyldiimidazole (28 mg, 0.17 mmol) were dissolved in dry THF (30 mL) and refluxed for 48 h. The reaction was then quenched with dd$H_2O$, concentrated under reduced pressure and the product was taken up with EtOAc. The organic layer was separated, washed with a brine solution, dried over anhydrous $Na_2SO_4$, filtered, and concentrated. Filtration over a pad of silica gel provided 159 mg of a yellow solid. ($C_{66}H_{85}N_{15}O_{17}$, 74%). $R_f$ = 0.38 ($SiO_2$, 5% MeOH/$Et_2O$). mp = 87 °C. HRMS (ESI): calcd for $(M+H)^+/z$, 1360.6318. Found 1360.6321. This yellow solid (159 mg, 0.117 mmol) was then dissolved in MeCN (5 mL) and treated with iodomethane (36 µL, 0.585 mmol). After stirring for 24 h at rt, the reaction mixture was concentrated under reduced pressure to afford **4** as a viscous yellow oil. ($C_{67}H_{88}N_{15}O_{17}I$, 148 mg, 92%). $^1$H NMR (400 MHz, DMSO-$d_6$) $\delta$ (ppm) 9.43 (1H, s), 7.85 (1H, s), 7.68 (1H, s), 7.41–7.30 (10H, m), 5.58 (4H, s), 4.55 (2H, br s), 4.35 (2H, br s), 3.89 (5H, br s), 3.74 (2H, br s), 3.41 (6H, s), 1.51 (18H, s), 1.26 (36H, br s). HRMS (ESI): calcd for $(M+H)^+/z$, 1374.6475. Found 1374.6477.

### Compound 7

A solution of *N*-Fmoc-ethylenediamine hydrochloride (25 mg, 0.078 mmol) and $Et_3N$ (22.0 µL, 0.156 mmol) in 1,2-dichloroethane (10 mL) was stirred for ca. 10 min after which **1** (50 mg, 0.078 mmol) and NaBH$(OAc)_3$ (21.5 mg, 0.101 mmol) were added. After stirring O/N, TLC and LCMS analysis revealed that the reaction was complete. An additional equivalent of **1** (50 mg, 0.078 mmol) and NaBH$(OAc)_3$ (21.5 mg, 0.101 mmol) were then added to the mixture, which was left to stir for a further 24 h at rt. The reaction was then quenched with dd$H_2O$ (10 mL) and the solvent was removed under reduced pressure. The resulting yellow residue was taken up in $Et_2O$ (20 mL), washed with brine (10 mL) and dried over anhydrous $Na_2SO_4$. Filtration, followed by silica gel flash chromatography (10% MeOH/$CH_2Cl_2$) yielded **7** ($C_{79}H_{98}N_{14}O_{18}$, 109 mg, 91%) as a pale yellow foam. $R_f$ = 0.79 ($SiO_2$, 10% MeOH/$CH_2Cl_2$). $^1$H NMR (400 MHz, $CDCl_3$) $\delta$ (ppm) 7.74–7.28 (19H, m), 5.57 (4H, s), 4.39 (4H, t, *J* = 7.2 Hz), 4.33 (2H, d, *J* = 7.3 Hz), 4.23 (1H, t, *J* = 7.3 Hz), 3.47 (6H, s), 3.38–3.26 (2H, m), 2.96 (4H, t, *J* = 7.2 Hz), 2.88 (2H, t, *J* = 5.6 Hz), 1.54 (18H, s), 1.32 (36H, s).$^{13}$C NMR (150 MHz, $CDCl_3$) $\delta$ (ppm) 165.6, 161.2, 161.0, 160.3, 156.5, 155.6, 152.5, 149.3, 144.1, 141.2, 134.9, 128.5, 127.5, 127.0, 125.2, 119.8, 92.8, 83.7, 82.9, 70.1, 66.5, 53.8, 50.8, 47.3, 41.2, 34.9, 28.1, 27.8. HRMS (ESI): calcd for $(M+H)^+/z$, 1531.7256. Found 1531.7253.

### Compound 8

A solution of *N*-Fmoc-butylenediamine hydrochloride (54.2 mg, 0.156 mmol) and $Et_3N$ (217 µL, 1.25 mmol) in 1,2-dichloroethane (15 mL) was stirred for ~10 min after which **1** (100 mg, 0.156 mmol) and NaBH$(OAc)_3$ (43.1 mg, 0.203 mmol) were added. After stirring O/N, TLC and LCMS showed that the reaction was complete. An additional equivalent of **1** (100 mg, 0.156 mmol) and NaBH$(OAc)_3$ (43.1 mg, 0.203 mmol) were then added to the mixture, which was left to stir for a further 24 h at rt. The reaction was then quenched with dd$H_2O$ (10 mL) and the solvent was removed under reduced pressure. The resulting yellow residue was taken up in $Et_2O$ (20 mL), washed with brine (10 mL), and dried over anhydrous $Na_2SO_4$. Filtration, followed by silica gel chromatography (0-10% MeOH/$CH_2Cl_2$) offered **8** ($C_{81}H_{102}N_{14}O_{18}$, 214 mg, 88%) as a pale yellow foam. $R_f$ = 0.45 ($SiO_2$, 5% MeOH/$CH_2Cl_2$). $^1$H NMR (500 MHz, $CDCl_3$) $\delta$ (ppm) 7.74–7.28 (19H, m), 5.57 (4H, s), 4.41 (4H, t, *J* = 7.3 Hz), 4.34 (2 H, d, *J* = 7.2 Hz), 4.21 (1H, t, *J* = 7.2 Hz), 3.48 (6H, s), 3.20–3.16 (2H, m), 2.93 (4H, t, *J* = 7.3 Hz), 2.78–2.62 (2H, m), 1.56 (18H, s), 1.60–1.52 (4H, m), 1.31 (36H, s).$^{13}$C NMR (125 MHz, $CDCl_3$) $\delta$ (ppm) 165.6, 161.2, 161.0, 160.3, 156.5, 155.6, 152.5, 149.3, 144.1, 141.2, 134.9, 128.5, 127.5, 127.0, 125.2, 119.8, 92.8, 83.7, 82.9, 70.0, 66.5, 53.8, 50.8, 47.3, 41.2, 35.0, 28.1, 27.8, 27.5, 24.9. HRMS (ESI): calcd for $(M+H)^+/z$, 1559.7569. Found 1559.7576.

### Compound 9

*N*-Boc ethylenediamine (44 mg, 0.27 mmol), **3** (100 mg, 0.273 mmol),[17] HBTU (103 mg, 0.273 mmol) and $Et_3N$ (72 µL, 0.52 mmol) were dissolved in DMSO (4 mL) and stirred at rt for 4 h. $Et_2O$ was then added to precipitate the product, which was collected, washed with $CH_2Cl_2$, and dried to provide **9** as a white solid ($C_{22}H_{31}N_5O_7S$, 107 mg, 77%). mp = 223.2 °C (decomposed). $^1$H NMR (500 MHz, DMSO-$d_6$) $\delta$ (ppm) 8.47 (1H, t, *J* = 5.3 Hz), 8.21 (1H, t, *J* = 6.6 Hz), 8.08 (1H, t, *J* = 5.9 Hz), 7.94–7.90 (2H, m), 7.78 (1H, t, *J* = 5.7 Hz), 7.72–7.68 (1H, m), 7.58–7.56 (2H, m), 6.78 (1H, t, *J* = 5.6 Hz), 3.88 (2H, s), 3.77 (2H, d, *J* = 5.6 Hz), 3.74 (2H, d, *J* = 5.7 Hz), 3.65 (2H, d, *J* = 5.9 Hz), 3.10–3.05 (2H, m), 3.00–2.90 (2H, m), 1.36 (9H, s). $^{13}$C NMR (150 MHz, DMSO-$d_6$) $\delta$ (ppm) 190.8, 169.6, 169.5, 169.3, 167.7, 156.1, 136.4, 134.5, 129.6, 127.3, 78.2, 43.0, 42.6, 42.5, 39.2, 32.9, 28.6. HRMS (ESI): calcd for $(M+Na)^+/z$ = 532.1836. Found 532.1834.

### Compound 10

TFA/thioanisole (1 mL, 95/5, v/v) was added to a solution of **9** (343 mg, 0.673 mmol) in $CH_2Cl_2$ (2 mL) at rt. After stirring for 1 h, the TFA was removed under reduced pressure. $Et_2O$ was then added to precipitate the product, which was washed with $Et_2O$ (3×) and $CH_2Cl_2$ (4×) to afford a pink solid ($C_{19}H_{24}F_3N_5O_7S$, 213 mg, 61%). This material (163 mg 0.313 mmol) was then dissolved in DMF (10 mL), treated with $Et_3N$ (132 μL, 0.964 mmol), and sonicated until it dissolved. Aldehyde **1** (400 mg, 0.625 mmol) was then added and the solution was stirred for ca. 10 min before the addition of $NaBH(OAc)_3$ (272 mg, 1.28 mmol). The mixture was stirred at rt for 24 h before the DMF was removed under reduced pressure. The viscous yellow residue was then dissolved in EtOAc, washed with $ddH_2O$, brine, and dried over anhydrous $Na_2SO_4$. Filtration, followed by silica gel flash chromatography (0–5% MeOH/DCM) offered the coupled adduct **10** as a solid ($C_{79}H_{103}N_{17}O_{21}S$, 269 mg, 51%). $R_f$ = 0.42 ($SiO_2$, 5% $MeOH/CH_2Cl_2$). mp = 88.8–89.3 °C. $^1H$ NMR (600 MHz, $CD_3OD$) $\delta$ (ppm) 7.88–7.31 (15H, m), 5.60 (4H, s), 4.32 (4H, t, $J$ = 7.3 Hz), 3.92 (4H, br s), 3.88–3.84 (4H, m), 3.44 (6H, s), 3.34–3.29 (2H, m), 2.93 (4H, t, $J$ = 7.0 Hz), 2.86 (2H, s), 2.82 (4H, t, $J$ = 7.3 Hz), 1.54 (18H, s), 1.28 (36H, s). $^{13}C$ NMR (150 MHz, $CD_3OD$) $\delta$ (ppm) 190.8, 170.8, 170.6, 170.1, 169.9, 165.8, 161.6, 160.9, 160.5, 156.2, 152.5, 149.3, 136.1, 135.0, 133.7, 128.7, 128.33, 128.32, 126.9, 92.9, 84.2, 83.0, 70.1, 51.3, 42.9, 42.5, 42.2, 41.5, 37.6, 35.5, 34.3, 32.1, 27.1, 26.7. HRMS (ESI): calcd for $(M+H)^+/z$ = 1658.7308. Found 1658.7315. Elemental analysis: Found: C 56.51; H 6.29; N 13.95; S 1.94. Calc. for $[C_{79}H_{103}N_{17}O_{21}S+CH_3OH]$: C, 56.83; H, 6.38; N, 14.08 S, 1.90.

### Compound 11

Compound **10** (200 mg, 0.121 mmol) was dissolved in 5 mL of 95% TFA/thioanisole (5 mL, v/v) and stirred at rt for 4 h. $Et_2O$ was then added to precipitate the product which was purified by extensive washing with $Et_2O$ and $CH_2Cl_2$ to afford **11** ($C_{35}H_{44}N_{17}O_9S$, 132 mg, 89%) as a white solid. mp = decomposed at 287 °C. $^1H$ NMR (600 MHz, DMSO-$d_6$+1 drop of $d$-TFA+$D_2O$) $\delta$ (ppm): 7.89–7.88 (2H, m), 7.68–7.66 (1H, m), 7.55–7.52 (2H, m), 4.40 (4H, br s), 3.84 (2H, s), 3.76 (2H, s), 3.72 (2H, s), 3.65 (2H, s), 3.59–3.54 (4H, m), 3.48–3.43 (4H, m), 2.91 (6H, br s). $^{13}C$ NMR (150 MHz, DMSO-$d_6$+one drop of $d$-TFA) $\delta$ (ppm): 190.8, 170.3, 169.8, 167.8, 162.4, 161.7, 160.2, 156.5, 156.0, 148.7, 136.3, 134.5, 129.6, 127.3, 82.9, 52.2, 49.9, 43.0, 42.6, 42.5, 40.4, 36.8, 32.9, 28.4. HRMS (MALDI): calcd for $(M+H)^+/z$ = 878.3223. Found 878.3224. Elemental analysis: Found: C, 39.77; H, 3.97; N, 18.88; S, 2.87. Calcd for $[C_{35}H_{44}N_{17}O_9S+(CF_3COOH)_3+H_2O]$: C, 39.78; H, 3.91; N, 19.23; S, 2.59.

### Compound 12

A mixture of 50:50 MeOH/DMF (2.5 mL) in a round bottom flask was degassed by bubbling argon for 30 min and then transferred to an argon filled round bottom flask containing a mixture of **11** (10.0 mg, 0.0082 mmol), $ReOCl_3(PPh_3)_2$ (14.5 mg, 0.016 mmol, 2 equiv), and $CH_3ONa$ (9.0 mg, 0.167 mmol, 20 equiv). The suspension was stirred at room temperature under positive argon pressure. After 30 min, the cloudy green solution turned into a cloudy brown color. Diethyl ether was then added which precipitated the brown complex immediately. The precipitate was then transferred with the solution into a centrifuge tube and centrifuged. The isolated solid was washed with diethyl ether (3×), hexane (3×), benzene (3×), chloroform (3×), $CH_2Cl_2$ (3×), and $ddH_2O$ (2×). The solid was then dried under vacuum to provide **12** ($C_{28}H_{35}N_{17}O_9SRe$, 8 mg, 94%). $^1H$ NMR (600 MHz, DMSO-$d_6$ + 1 drop of TFA-$d$) $\delta$ (ppm): 4.45–4.43 (4 H, m), 4.18–4.10 (2H, m), 3.81 (2H, s), 3.78–3.75 (2H, m), 3.72–3.70 (2H, m), 3.59 (4H, br s), 3.53–3.47 (4H, m), 2.96 (6H, br s). Low Resolution LC–MS: calcd for $(M+2H)^+/z$ = 974.2. Found 974.3. HRMS (MALDI): calcd for $(M+2H)^+/z$ = 974.2238. Found 974.2234. IR: 1634 (C=O amide), 1531 (C=N), 973.0 (Re=O). Elemental analysis: Found: C, 35.00; H, 4.47; N, 22.86. Calcd for $[C_{28}H_{35}N_{17}O_9ReS^- + 2MeOH]$: C, 34.78; H, 4.18; N, 22.98.

## Acknowledgments

We thank the National Research Council of Canada (NRC), the University of Alberta, and the Natural Science and Engineering Research Council (NSERC) for supporting this research program. A.A. thanks Alberta Innovates for the Alberta Innovates Graduate Student Scholarship in Nanotechnology.

## Supplementary data

Supplementary data associated with this article can be found, in the online version, at doi:10.1016/j.tetlet.2012.01.090.

## References and notes

1. (a) Fenniri, H.; Deng, B. L.; Ribbe, A. E. *J. Am. Chem. Soc.* **2002**, *124*, 11064–11072; (b) Moralez, J. G.; Raez, J.; Yamazaki, T.; Motkuri, R. K.; Kovalenko, A.; Fenniri, H. *J. Am. Chem. Soc.* **2005**, *127*, 8307–8309; (c) Fenniri, H.; Deng, B. L.; Ribbe, A. E.; Hallenga, K.; Jacob, J.; Thiyagarajan, P. *Proc. Natl. Acad. Sci. U.S.A.* **2002**, *99*, 6487–6492; (d) Raez, J.; Moralez, J. G.; Fenniri, H. *J. Am. Chem. Soc.* **2004**, *126*, 16298–16299; (e) Fenniri, H.; Mathivanan, P.; Vidale, K. L.; Sherman, D. M.; Hallenga, K.; Wood, K. V.; Stowell, J. G. *J. Am. Chem. Soc.* **2001**, *123*, 3854–3855; (f) Beingessner, R. L.; Deng, B.-L.; Fanwick, P. E.; Fenniri, H. *J. Org. Chem.* **2008**, *73*, 931–939; (g) Tikhomirov, G.; Oderinde, M.; Makeiff, D.; Mansouri, A.; Liu, W.; Heirtzler, F. R.; Kwok, D. Y.; Fenniri, H. *J. Org. Chem.* **2008**, *73*, 4248–4251.
2. Beingessner, R. L.; Diaz, J. A.; Hemraz, U. D.; Fenniri, H. *Tetahedron Lett.* **2011**, *52*, 661–664.
3. (a) Borzsonyi, G.; Beingessner, R. L.; Yamazaki, T.; Cho, J.-Y.; Myles, A. J.; Malac, M.; Egerton, R.; Kawasaki, M.; Ishizuka, K.; Kovalenko, A.; Fenniri, H. *J. Am. Chem. Soc.* **2010**, *132*, 15136–15139; (b) Borzsonyi, G.; Johnson, R. S.; Myles, A. J.; Cho, J.-Y.; Yamazaki, T.; Beingessner, R. L.; Kovalenko, A.; Fenniri, H. *Chem. Comm.* **2010**, *46*, 6527–6529; (c) Borzsonyi, G.; Alsbaiee, A.; Beingessner, R. L.; Fenniri, H. *J. Org. Chem.* **2010**, *75*, 7233–7239.
4. (a) Chun, A. L.; Moralez, J. G.; Webster, T. J.; Fenniri, H. *Biomaterials* **2005**, *26*, 7304–7309; (b) Chun, A. L.; Moralez, J. G.; Fenniri, H.; Webster, T. J. *Nanotechnology* **2004**, *15*, S234–S239; (c) Zhang, L.; Rodriguez, J. R.; Myles, A. J.; Fenniri, H.; Webster, T. J. *Nanotechnology* **2009**, *20*, 175101 (12 p).; (d) Zhang, L.; Rakotondradany, F.; Myles, A. J.; Fenniri, H.; Webster, T. J. *Biomaterials* **2009**, *30*, 1309–1320; (e) Zhang, L.; Ramsaywack, S.; Fenniri, H.; Webster, T. J. *Tissue Eng., Part A.* **2008**, *14*, 1353–1364; (f) Suri, S. S.; Rakotondradani, F.; Myles, A. J.; Fenniri, H.; Singh, B. *Biomaterials* **2009**, *30*, 3084–3090; (g) Zhang, L.; Chen, Y.; Rodriguez, J.; Fenniri, H.; Webster, T. J. *Int. J. Nanomedicine* **2008**, *3*, 323–333; (h) Chen, Y.; Pareta, R. A.; Bilgen, B.; Myles, A. J.; Fenniri, H.; Ciombor, D. M.; Aaron, R. K.; Webster, T. J. *Tissue Eng. Part C* **2010**, *16*, 1233–1243; (i) Zhang, L.; Hemraz, U. D.; Fenniri, H.; Webster, T. J. *J. Biomed. Mater. Res. A* **2010**, *95A*, 550–563.
5. Fine, E.; Zhang, L. J.; Fenniri, H.; Webster, T. J. *Int. J. Nanomedicine* **2009**, *4*, 91–97.
6. Alshamsan, A.; El-Bakkari, M.; Fenniri, H. *Mater. Res. Soc. Symp. Proc.* **2010**, *2011*, 1316–1319.
7. Chen, Y.; Song, S.; Yan, Z.; Fenniri, H.; Webster, T. J. *Int. J. Nanomedicine* **2011**, *6*, 1035–1044.
8. Song, S.; Chen, Y.; Yan, Z.; Fenniri, H.; Webster, T. J. *Int. J. Nanomedicine* **2011**, *6*, 101–107.
9. Chhabra, R.; Moralez, J. G.; Raez, J.; Yamazaki, T.; Cho, J.-Y.; Myles, A. J.; Kovalenko, A.; Fenniri, H. *J. Am. Chem. Soc.* **2010**, *132*, 32–33.
10. (a) Mol, J. C. *Catalysis Today* **1999**, *51*, 289–299; (b) Jiang, Y.; Hess, J.; Fox, T.; Berke, H. *J. Am. Chem. Soc.* **2010**, *132*, 18233–18247; (c) Umeda, R.; Kaiba, K.; Tanaka, T.; Takahashi, Y.; Nishimura, T.; Nishiyama, Y. *Synlett* **2010**, 3089–3091.
11. (a) Fritzberg, A. R.; Kasina, S.; Eshima, D.; Johnson, D. L. *Nucl. Med.* **1986**, *27*, 111–116; (b) Roberts, J.; Chen, B.; Curtis, L. M.; Agarwal, A.; Sanders, P. W.; Zinn, K. R. *Am. J. Physiol. Renal Physiol.* **2007**, *293*, F1408–F1412; (c) Reyes, L.; Navarrete, M. *J. Radioanal. Nucl. Ch.* **2002**, *251*, 245–248; (d) Itoh, K.; Matsui, Y.; Kato, C.; Mochizuki, T.; Kitabatake, A. *Ann. Nucl. Med.* **1996**, *10*, 251–255; (e) Taylor, A.; Eshima, D., Jr.; Fritzberg, A. R.; Christian, P. E.; Kasina, S. *J. Nucl. Med.* **1986**, *27*, 795–803; (f) Itoh, K. *Ann. Nucl. Med.* **2001**, *15*, 179–190; (g) Wang, Y.; Liu, X.; Hnatowich, D. J. *Nature Protocols* **2007**, *2*, 972–978.
12. Pimlott, S. L.; Sutherland, A. *Chem. Soc. Rev.* **2011**, *40*, 149–162.
13. Dilworth, J. R.; Parrott, S. J. *Chem. Soc. Rev.* **1998**, *27*, 43–55.
14. (a) de Barros, A. L. B.; Cardoso, V. N.; Mota, L. G.; Leite, E. A.; Oliveira, M. C.; Alves, R. J. *Bioorg. Med. Chem. Lett.* **2010**, *20*, 2478–2480; (b) de Barros, A. L. B.; Cardoso, V. N.; Mota, L. G.; Alves, R. J. *Bioorg. Med. Chem. Lett.* **2010**, *20*, 315–317; (c) de Barros, A. L. B.; Cardoso, V. N.; Mota, L. G.; Leite, E. A.; de Oliveira, M. C.; Alves, R. J. *Bioorg. Med. Chem. Lett.* **2009**, *19*, 2497–2499.
15. Reyes, L.; Navarrete, M. *J. Radioanal. Nucl. Chem.* **2002**, *251*, 245–248.
16. Kang, L.; Wang, R. F.; Yan, P.; Liu, M.; Zhang, C. L.; Yu, M. M.; Cui, Y. G.; Xu, X. J. *J. Nucl. Med.* **2010**, *51*, 978–986.
17. Brandau, W.; Bubeck, B.; Eisenhut, M.; Taylor, D. M. *Int. J. Radiat. Appl. Instrum. Part A.* **1988**, *39*, 121–129.

18. Guhlke, S.; Schaffland, A.; Zamora, P. O.; Sartor, J.; Diekmann, D.; Bender, H.; Knapp, F. F.; Biersack, H.-J. *Nucl. Med. Biol.* **1998**, *25*, 621–631.
19. (a) Riddoch, R. W.; Schaffer, P.; Valliant, J. F. *Bioconjugate Chem.* **2006**, *17*, 226–235; (b) Aufort, M.; Gonera, M.; Chaignon, N.; Le Clainche, L.; Dugave, C. *Eur. J. Med. Chem.* **2009**, *44*, 3394–3401.
20. The perrhenate (ReO4)- anion is very stable and often used to introduce rhenium to bioactive compounds through in situ reduction. For references see (a) Zamora, P. O.; Marek, M. J.; Knapp, F. F., Jr. *Appl. Radiat. Isot.* **1997**, *48*, 305–309; (b) Das, T.; Banerjee, S.; Samuel, G.; Kothari, K.; Unni, P. R.; Sarma, H. D.; Ramamoorthy, N.; Pillai, M. R. A. *Nucl. Med. Biol.* **2000**, *27*, 189–197; (c) Rose, D. J.; Maresca, K. P.; Nicholson, T.; Davison, A.; Jones, A. G.; Babich, J.; Fischman, A.; Graham, W.; DeBord, J. R.; Zubieta, J. *Inorg. Chem.* **1998**, *37*, 2701–2716.
21. Zervas, L.; Photaki, I.; Ghelis, N. *J. Am. Chem. Soc.* **1963**, *85*, 1337–1341.